Research Article

Check for updates

Vitamin D receptor (VDR) mediates the quiescence of activated hepatic stellate cells (aHSCs) by regulating M2 macrophage exosomal smooth muscle cell-associated protein 5 (SMAP-5)

Xuwentai LIU, Yue WU, Yanyi LI, Kaiming LI, Siyuan HOU, Ming DING, Jingmin TAN, Zijing ZHU, Yingqi TANG, Yuming LIU, Qianhui SUN, Cong WANG✉, Can ZHANG✉

State Key Laboratory of Natural Medicines / Jiangsu Key Laboratory of Drug Discovery for Metabolic Diseases / Center of Advanced Pharmaceuticals and Biomaterials, China Pharmaceutical University, Nanjing 210009, China

Abstract: An effective therapeutic regimen for hepatic fibrosis requires a deep understanding of the pathogenesis mechanism. Hepatic fibrosis is characterized by activated hepatic stellate cells (aHSCs) with an excessive production of extracellular matrix. Although promoted activation of HSCs by M2 macrophages has been demonstrated, the molecular mechanism involved remains ambiguous. Herein, we propose that the vitamin D receptor (VDR) involved in macrophage polarization may regulate the communication between macrophages and HSCs by changing the functions of exosomes. We confirm that activating the VDR can inhibit the effect of M2 macrophages on HSC activation. The exosomes derived from M2 macrophages can promote HSC activation, while stimulating VDR alters the protein profiles and reverses their roles in M2 macrophage exosomes. Smooth muscle cell-associated protein 5 (SMAP-5) was found to be the key effector protein in promoting HSC activation by regulating autophagy flux. Building on these results, we show that a combined treatment of a VDR agonist and a macrophage-targeted exosomal secretion inhibitor achieves an excellent anti-hepatic fibrosis effect. In this study, we aim to elucidate the association between VDR and macrophages in HSC activation. The results contribute to our understanding of the pathogenesis mechanism of hepatic fibrosis, and provide potential therapeutic targets for its treatment.

Key words: Hepatic fibrosis; Hepatic stellate cell (HSC); Macrophage; Exosome; Vitamin D receptor (VDR); Smooth muscle cell-associated protein 5 (SMAP-5)

1 Introduction

Hepatic fibrosis is a common pathological process of many chronic liver diseases caused by continuous liver damage (Pellicoro et al., 2014). The morbidity of hepatic fibrosis caused by various etiologies is increasing rapidly all over the world (Mokdad et al., 2014). Although there has been great progress in the treatment of hepatic fibrosis, an effective treatment is still lacking because of the poor therapeutic effect or serious side effects of the drugs currently on the market (Kisseleva and Brenner, 2021). Activated

✉ Can ZHANG, zhangcan@cpu.edu.cn
Cong WANG, wangcong@cpu.edu.cn

ⓘ Can ZHANG, https://orcid.org/0000-0003-3529-5438
Cong WANG, https://orcid.org/0000-0001-8241-807X

hepatic stellate cells (aHSCs) are the primary effector cells for hepatic fibrosis. They can transform into myofibroblast-like cells and produce a large amount of extracellular matrix in response to various liver injuries (Yin et al., 2013; Cai et al., 2022). Growing evidence indicates that reversing the activation status of HSCs to quiescence could contribute to the regression of hepatic fibrosis (Lu et al., 2021; Shen et al., 2022). Thus, a more detailed understanding of the underlying mechanism of HSC activation might provide potential targets for novel antifibrosis therapy.

Macrophages, including those derived from monocytes in blood circulation and inherent Kupffer cells, also play critical roles in hepatic fibrosis (Seki and Schwabe, 2015; Bernsmeier et al., 2020). The predominant M2 macrophages in the injured liver have been shown to promote the proliferation and activation of HSCs (Sica et al., 2014; Sun et al., 2017).

Therefore, hindering macrophage polarization to M2 phenotypes would be beneficial for the suppression of HSC activation.

Previous studies have shown that the vitamin D receptor (VDR), the main molecule enabling vitamin D to exert its biological function, participates in regulating macrophage polarization (Liu et al., 2006; Zhou et al., 2020). VDR is highly expressed in macrophages, and activation of liver macrophage VDR can ameliorate liver inflammation, steatosis, and insulin resistance (Dong et al., 2020). Moreover, vitamin D deficiency is common in patients with hepatic fibrosis (Konstantakis et al., 2016), and regulation of VDR activity is involved in the development of hepatic fibrosis (Ding et al., 2013; Duran et al., 2016; Wang et al., 2020). Considering the significance of VDR in the regulation of macrophage activity, we wondered whether VDR may regulate macrophages and thus affect the activation of HSCs, as well as how we might modulate their communication. Exosomes, extracellular vesicles derived from various cells, usually serve as a communicator among cells via their harbored cargos including proteins, RNAs, and DNAs (Thery et al., 2018; Kalluri and LeBleu, 2020; Shen et al., 2022). Due to the diverse composition and higher loading, the exact underlying role of protein in the exosomes that mediate the communication between macrophages and HSCs, especially after the regulation of VDR, remains unclear.

Herein, we proposed to elucidate the role of the VDR of M2 macrophages in HSC activation involving regulation of the protein profile of exosomes derived from macrophages. The results contribute to the understanding of the underlying mechanism of HSC activation in fibrotic microenvironments with abundant M2 macrophages, thus offering potential targets and promising strategies for the treatment of hepatic fibrosis.

2 Materials and methods

2.1 Isolation of primary cells

Primary Kupffer cells were isolated from 8-week-old male C57BL/6J mice by sequential pronase and collagenase IV digestion, followed by density gradient centrifugation. In detail, after anesthesia with pentobarbital sodium (3 mg/kg body weight), the mouse liver was perfused with Hank's balanced salt solution (HBSS) via the portal vein, and then perfused sequentially with pronase (0.05%, mass fraction) and collagenase IV (0.05%, mass fraction). After digestion, the liver was mashed ex vivo in a dish, incubated at 37 ℃ in HBSS containing 0.05% (mass fraction) collagenase IV and 2% (mass fraction) deoxyribonuclease. The suspension was then centrifuged at $50g$ for 3 min to separate non-parenchymal cells from hepatocytes and cellular debris. Kupffer cells were collected by density gradient centrifugation in 25% over 50% (volume ratio) Percoll. The cells were then re-suspended in Roswell Park Memorial Institute (RPMI)-1640 medium containing 10% (volume fraction) fetal bovine serum (FBS) and 1% (volume fraction) Pen-Strep. After culturing for 4 h, the medium was changed to remove non-adherent cells. Primary HSCs were isolated using a single-step Percoll gradient as previously reported, after anesthesia and in situ perfusion by pronase/collagenase IV (Qu et al., 2018). Isolated HSCs were then cultured in RPMI-1640 medium containing 10% FBS and 1% Pen-Strep for 40 h prior to end-point assays.

2.2 Polarization of THP-1 and primary Kupffer cells

THP-1 cells were differentiated to M0 macrophage, an adherent phenotype, by treatment with 50 nmol/L phorbol 12-myristate 13-acetate (PMA) for 72 h. THP-1-derived M0 macrophages and primary Kupffer cells were stimulated by co-supplementation of 200 ng/mL lipopolysaccharide (LPS) and 100 ng/mL interferon-γ (IFN-γ) for 24 h to polarize towards the M1 phenotype, or 20 ng/mL interleukin-4 (IL-4) for 24 h to polarize towards the M2 phenotype (Li et al., 2022). The macrophages were then cultured with 20 μmol/L GW4869 for 24 h to inhibit exosome secretion.

2.3 Isolation and polarization of human peripheral blood-derived macrophages

Once human blood samples were obtained, gradient centrifugation was performed using human peripheral blood cell separation solution to isolate the peripheral blood mononuclear cells (PBMCs). After centrifugation, the interface between the plasma (top) and red (bottom) layer was collected carefully and used for the isolation of monocytes. Then the PBMCs were resuspended in serum-free RPMI-1640, counted,

and adjusted to a concentration of 1×10^7 cells/mL. After 4 h, non-adherent cells were carefully washed away with warm phosphate-buffered saline (PBS), and then the adherent cells were cultured for 5 d in RPMI-1640 supplemented with 15% FBS and 20 ng/mL macrophage colony-stimulating factor (M-CSF).

2.4 Exosome isolation and purification

Exosomes were isolated using an Exosome Concentration kit, in accordance with the manufacturer's instructions. Briefly, after centrifugation at 3000g for 10 min to eliminate dead cells and cell debris, conditioned medium was mixed with binding buffer at 10:1 (volume ratio). Binding resin was added and mixed gently for 15 min, and then the suspension was spun at 3000g for 2 min. The supernatant was then discarded and the pellets were transferred into spin columns, re-suspended in washing buffer, and spun once again as above. The final pellet was re-suspended in elution buffer, and centrifuged at 3000g for 2 min. The filtrate was a concentrated exosome solution.

2.5 Mass spectrometry-based proteomics

Extracted peptides (six fractions per sample) were analyzed using nanoscale liquid chromatography coupled to tandem mass spectrometry (nanoLC-MS/MS) in a Thermo Fisher Orbitrap Fusion system (Thermo Scientific, USA). Samples were analyzed using acquisition strategies. Specifically, sequential collision-induced dissociation (CID)-electron transfer dissociation (ETD)-MS2 acquisition was performed to MS1 precursor in a CID-MS2-MS3-ETD-MS2 approach. Mass difference-dependent CID-MS3 acquisitions were triggered subsequently if a unique mass difference in the CID-MS2 spectrum was observed. Calibrated charge-dependent ETD parameters were enabled.

2.6 Short hairpin RNA (shRNA) transfection in vivo

Adeno-associated virus-mediated shRNA (AAV-shRNA; GeneChem, Shanghai, China) was applied to hepatic fibrosis model mice at 9.33×10^{12} vector genomes (v. g)/kg body weight by vein injection. Mice were sacrificed after four weeks.

2.7 Statistical analysis

Statistical analyses were performed using GraphPad Prism 8.0.1 software. All graphical data are presented as mean±standard error of mean (SEM). Statistical significance was determined using two-tailed Student's t-tests or one-way analysis of variance (ANOVA).

3 Results

3.1 Regulation of the polarization of macrophages by VDR, leading to suppression of HSC activation

To explore the role of VDR in the polarization of macrophages, the expression levels of VDR and its target genes in THP-1-derived M0, M1, and M2 macrophages were determined by western blot and reverse transcription-polymerase chain reaction (RT-PCR) (Figs. 1a, S1a, and S1b; primer sequences for RT-PCR were listed in Table S1; cell lines and cell polarization reagents were listed in supplementary methods). Compared to that of M0 macrophages, the expression of VDR was decreased in M2 macrophages. Then to confirm that the activation of VDR can influence the polarization of macrophages, THP-1-derived macrophages were treated with calcipotriol (50 nmol/L), a kind of VDR agonist, and the expression levels of M1 and M2 macrophage biomarkers, cluster of differentiation 86 (CD86) and CD206, were detected by flow cytometry analysis. After treatment with calcipotriol, CD206 was significantly down-regulated in M2 macrophages while CD86 was slightly up-regulated in M1 macrophages (Fig. 1b). Besides, the polarization from M0 to M2 was significantly inhibited after treatment with calcipotriol (Fig. S1c).

It has been proved that there is interaction between macrophages and HSCs (Chen et al., 2020; Hu et al., 2021). We also found that clophosome-mediated macrophage depletion suppressed collagen accumulation in hepatic fibrosis mice (Fig. S1d). To investigate the effects of different polarization state macrophages on the activation of HSCs, conditioned media of M0, M1, and M2 macrophages were each co-cultured with human HSC line, LX-2. Cell counting kit-8 (CCK-8) assay showed a remarkably promoted proliferation of LX-2 cells cultured in M2 macrophage-conditioned medium, which was suppressed by calcipotriol, suggesting that activation of VDR might inhibit the function of M2 macrophages (Fig. 1c, the method of CCK-8 assay was listed in supplementary methods). Beside the proliferation, the expression levels of collagen I and α-smooth muscle actin (α-SMA) were also obviously
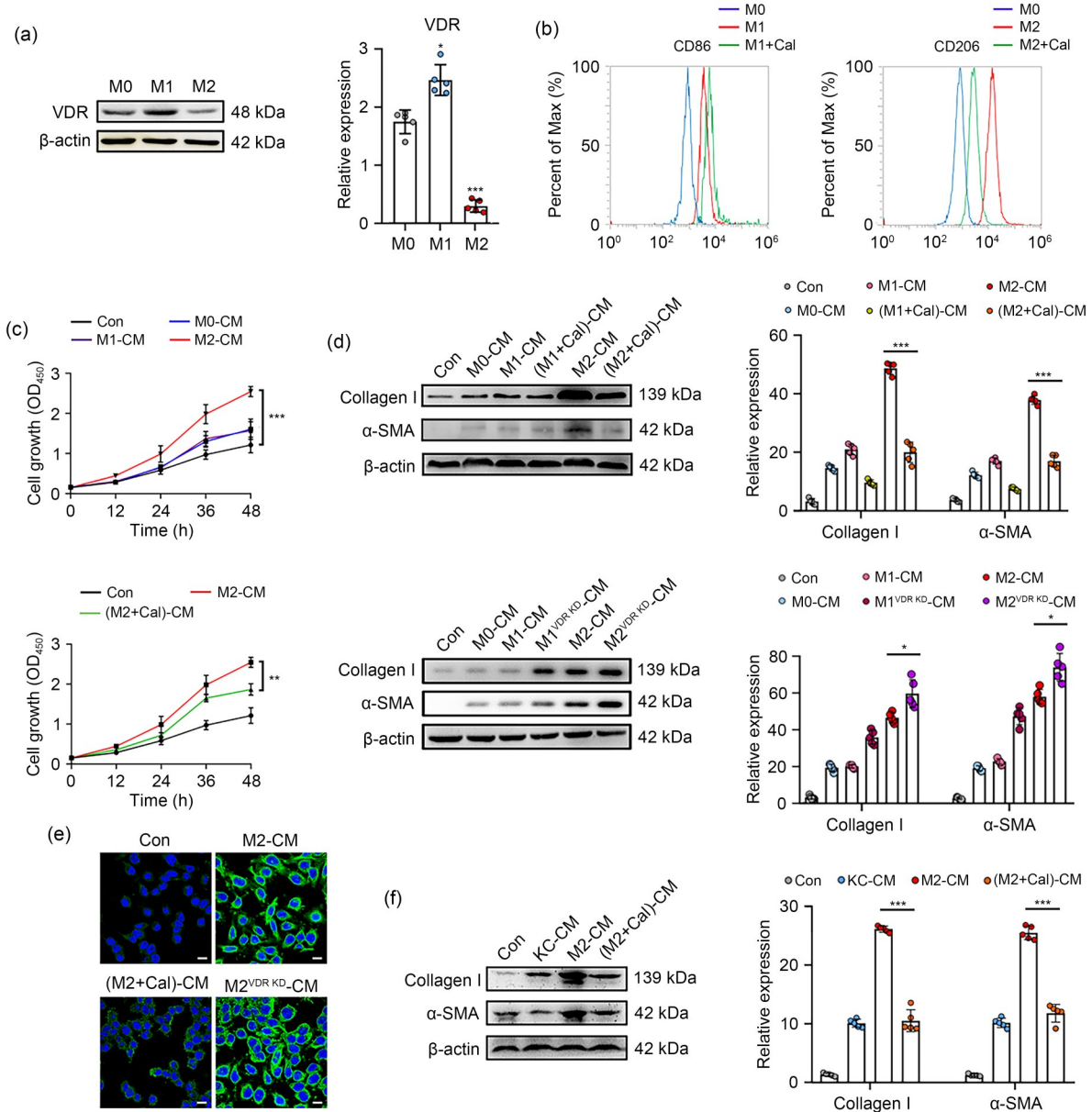
Fig. 1 Effect of VDR on the polarization of macrophages, leading to suppression of HSC activation. (a) Expression of VDR in different phenotypes of macrophages was examined by western blot. Representative gel electrophoresis bands are shown. Protein expression levels were quantified by densitometry and normalized to the expression of β-actin. Data are expressed as mean±SEM (*n*=5). * *P*<0.05, ** *P*<0.01, *** *P*<0.001. The same method of quantification and data expression were used in (c), (d), and (f). **(b)** Flow cytometry analyses of CD86 in THP-1-derived M0 and M1 and calcipotriol-treated M1 macrophages, and CD206 in THP-1-derived M0 and M2 and calcipotriol-treated M2 macrophages. **(c)** Cell growth curves of LX-2 cultured in control medium, THP-1-derived M0-, M1-, and M2-conditioned media (upper curve), and cell growth curves of LX-2 cultured in control medium, THP-1-derived M2-conditioned medium and calcipotriol-treated M2-conditioned medium (lower curve). Data are expressed as mean±SEM (*n*=6). **(d)** Expression of collagen I and α-SMA in LX-2 co-cultured with different macrophages was examined by western blot. Representative gel electrophoresis bands are shown (*n*=5). **(e)** CLSM images of LX-2 cultured in different conditioned media, co-stained for α-SMA (green) and Hoechst (blue), showed activation of LX-2. Scale bar=5 μm. **(f)** Expression of collagen I and α-SMA in primary HSCs co-cultured with different macrophages was examined by western blot. Representative gel electrophoresis bands are shown (*n*=5). VDR: vitamin D receptor; HSC: hepatic stellate cell; SEM: standard error of mean; CD86: cluster of differentiation 86; Cal: calcipotriol; Max: maximum; Con: control; CM: conditioned medium; OD_{450}: optical density at 450 nm; α-SMA: α-smooth muscle actin; KD: knockdown; CLSM: confocal laser scanning microscope; KC: Kupffer cell (Note: for interpretation of the references to color in this figure legend, the reader is referred to the web version of this article).

raised in LX-2 cells after treatment with M2 macrophage-conditioned medium (Figs. 1d and S1e). These results suggested that the HSCs become highly activated when co-cultured with M2 macrophages.

To further confirm that VDR participates in HSC activation by macrophages, M1 and M2 macrophages were treated with calcipotriol to activate VDR, or with transfected small interfering RNA (siRNA) to knock down *VDR*, and then co-cultured with HSCs. LX-2 activation was inhibited after co-culturing with calcipotriol-treated M2 macrophages, but further increased after co-culturing with *VDR*-knockdown M2 macrophages (Figs. 1d, 1e, and S1e–S1g). Similar results were also found in the primary HSCs and Kupffer cells isolated from C57BL/6 mice by single-step Percoll gradient, after in situ perfusion by pronase/collagenase IV (Fig. 1f).

In summary, these results suggested that macrophages, especially the M2 phenotype, promote the activation of HSCs, and this effect can be down-regulated by VDR activation.

3.2 Regulation of the activation of HSCs by exosomes derived from macrophages

Exosomes were isolated from macrophage-conditioned medium using an Exosome Concentration kit, at a concentration of 7.38×10^9 particles/g and with an average size of (136.9 ± 58.7) nm (Fig. 2a). The dynamics of 1,1'-dioctadecyl-3,3,3',3'-tetramethylindodicarbocyanine, 4-chlorobenzenesulfonate salt (DiD)-labeled macrophage-derived exosomes internalized by LX-2 cells was visualized and quantified (Fig. S2a), proving that exosomes released by macrophages can be absorbed by HSCs.

To confirm the regulatory effect of macrophage-derived exosomes on HSC activation, LX-2 cells were treated with exosomes isolated from conditioned medium of THP-1-derived M0, M1, and M2 macrophages. The CCK-8 assay showed that the proliferation of LX-2 cells co-cultured with M2 exosomes was significantly increased (Fig. 2b). The expression of collagen I and α-SMA was also noticeably increased (Figs. 2c, S2c, and S2d). GW4869 is a neutral sphingomyelinase inhibitor preventing the formation of intraluminal vesicles, and is widely accepted as being able to block exosome production. When LX-2 cells were co-cultured with M2 macrophages treated with GW4869, the increased cell proliferation and activation were both significantly inhibited (Figs. 2b–2d, S2g, and S2h); the non-cytotoxic assay of GW4869 is shown in Fig. S2b. Then, M0 and M2 macrophage-conditioned media were collected and ultracentrifuged at $100\,000g$ for 70 min to obtain exosome-free conditioned medium. After treatment with M2-conditioned medium with depleting of exosomes (M2-dExo), the activation of LX-2 cells was significantly inhibited compared with the full-component conditioned medium (Figs. S2e and S2f), confirming that M2 macrophage exosomes mediate the pro-activation of HSCs.

Moreover, since M2 macrophage exosomes mediated the pro-activation of HSCs, activating the VDR of M2 macrophages could block this interaction and inhibit HSC activation. This confirmed that the VDR pathway is non-redundantly upstream of exosome-mediated signaling to HSCs (Fig. S2i). When exosomes were removed by ultracentrifugation, the activation of HSCs was also inhibited although calcipotriol was not present. The same results were found in primary Kupffer cells and primary HSCs isolated from mouse liver (Figs. 2c and S2j), as well as in human PBMCs (Fig. S3).

Next, to verify the important role of macrophage exosomes in vivo, GW4869 (2.5 mg/kg body weight) was given to mice to inhibit the secretion of exosomes. Liposomes were used as GW4869 carriers due to their unique properties of retention in the liver and being absorbed mostly by liver macrophages. As illustrated in the treatment schedule (Fig. S4a), GW4869 encapsulated in liposome (GWLP) was intravenously injected (i.v.) into carbon tetrachloride (CCl_4)-induced hepatic fibrosis mice. The VDR agonist calcipotriol (20 μg/kg body weight) was administered by oral gavage. The distribution of GWLP showed co-localization with CD206-positive macrophages in the liver (Fig. S4b). After the mice were sacrificed and the corresponding detection performed, the results showed that treatment with calcipotriol or GWLP alone showed significant inhibition of collagen I and α-SMA expression, while after combined treatment, the fibrosis was much more inhibited (Fig. 2e). Meanwhile, the calcipotriol and GWLP combined treatment showed better repair of liver tissue structure, as shown by hematoxylin and eosin (H&E) staining, more decreased collagen deposition, as shown by Masson's trichrome staining, and down-regulated α-SMA protein expression, as shown by immunofluorescence analysis (Figs. 2f, S4c, and
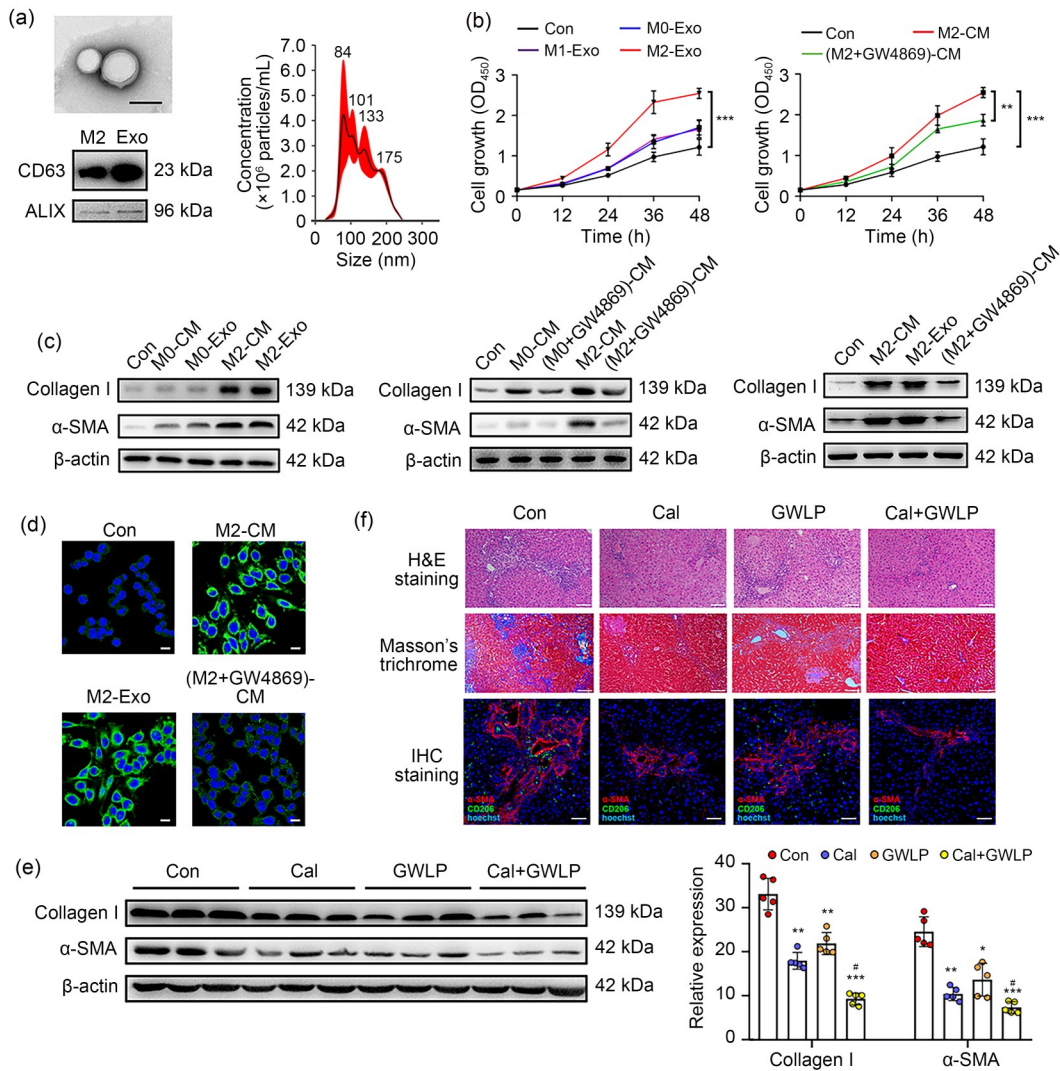
Fig. 2 Regulation of the activation of HSCs by exosomes derived from macrophages. (a) Electron microscope images, representative western blots of CD63 and ALIX, and nanoparticle tracking analysis of macrophage exosomes, purified with an Exosome Concentration kit. Representative gel electrophoresis bands are shown (*n*=3). Scale bar=100 nm. The method of nanoparticle tracking analysis was listed in supplementary methods. **(b)** Cell growth curves of LX-2 treated with control medium, M0-, M1-, and M2-derived exosomes (left). Cell growth curves of LX-2 cultured in control medium, M2-conditioned medium, and GW4869-treated M2-conditioned medium (right). Data are expressed as mean± SEM (*n*=6). **(c)** Expression of collagen I and α-SMA in LX-2 treated with different macrophage exosomes or conditioned medium was examined by western blot (left two sets). Expression of collagen I and α-SMA in primary HSCs was examined by western blot (right). Representative gel electrophoresis bands are shown. **(d)** CLSM images of LX-2 cultured in different conditioned media, co-stained for α-SMA (green) and Hoechst (blue), showed activation of LX-2. Scale bar=5 μm. **(e)** Detection of protein expression with western blot analysis of collagen I and α-SMA in liver samples from different treated CCl₄ model mice (left). β-Actin was used as the control. Gray scale analysis was performed and quantification of collagen I/β-actin and α-SMA/β-actin is shown (right). Data are expressed as mean±SEM (*n*=5). **(f)** Calcipotriol and GWLP inhibited the development of CCl₄-induced liver lesions, collagen deposition, and α-SMA expression. Liver lesions were detected by H&E staining and collagen deposition by Masson's trichrome staining. α-SMA expression was determined by immunofluorescence. H&E and Masson's trichrome stain: scale bar=200 μm. CLSM images: co-stained for α-SMA (red) and Hoechst (blue); scale bar=50 μm. * *P*<0.05, ** *P*<0.01, *** *P*<0.001 vs. Con. # *P*<0.05 vs. Cal. HSCs: hepatic stellate cells; CD63: cluster of differentiation 63; Exo: exosome; ALIX: antilymphocytic globulin 2-interacting protein X; SEM: standard error of mean; Con: control; CM: conditioned medium; OD₄₅₀: optical density at 450 nm; α-SMA: α-smooth muscle actin; CLSM: confocal laser scanning microscope; Cal: calcipotriol; GWLP: GW4869 encapsulated in liposome; CCl₄: carbon tetrachloride; H&E: hematoxylin and eosin; IHC: immunohistochemistry (Note: for interpretation of the references to color in this figure legend, the reader is referred to the web version of this article).

S4d). Moreover, the combination of calcipotriol and GWLP treatment showed stronger inhibition of alanine aminotransferase (ALT), aspartate aminotransferase (AST), and total bile acid (TBA) (Fig. S4e). Similar results were found in bile duct ligation (BDL) mice (Figs. S5a–S5e). There was no effect on serum calcium in mice (Fig. S5f), suggesting that this combination has no hypercalcemic effects in vivo.

To summarize, we demonstrated that M2 macrophages promote the activation of HSCs by exosomes and that activating VDR or blocking the secretion of macrophage exosomes can inhibit HSC activation and hepatic fibrosis in vitro and in vivo.

3.3 Proteomic analysis of SMAP-5 as an HSC-activating factor

To explore the mechanisms of VDR regulation of HSC activation through macrophage exosomes, the total proteins in exosomes derived from M0, M2, and calcipotriol-treated M2 macrophages were isolated, at the amount of 1×10^8 of each group. Using LC-MS/MS analysis, 5520 proteins were identified. The results showed that 105 proteins were over-expressed by at least 2-fold in M2 macrophage-derived exosomes compared with those derived from M0 macrophages. Also, 64 proteins were at least half down-regulated in exosomes derived from calcipotriol-treated M2 macrophages compared with those derived from M2 macrophages (Fig. 3a). By merging these two screening results using Venn diagram analysis, 54 proteins were obtained in the intersection (Fig. 3b), suggesting that these may be key proteins that can promote the activation of HSCs.

A heatmap analysis of these 54 intersection proteins was performed. We found that smooth muscle cell-associated protein 5 (SMAP-5) was the most differentially expressed protein. Its expression was 12-fold higher in M2 macrophage-derived exosomes than in M0-derived exosomes ($P=0.0002$) and was significantly down-regulated after calcipotriol treatment ($P=0.0027$) (Fig. 3c). This proteomic data were confirmed by western blot (Fig. 3d), which was consistent with the LC-MS/MS results (Fig. 3e).

Next, the effect of SMAP-5 on HSC activation was examined. After transfection with SMAP-5-over-expressed plasmids in LX-2 cells, the expression levels of collagen I and α-SMA were both up-regulated (Fig. 3f). Also, after *SMAP-5* was knocked down

using SMAP-5-specific siRNA (siSMAP-5) in LX-2 cells, the activation caused by transforming growth factor-β (TGF-β) was significantly reduced (Fig. 3f).

These results suggested that SMAP-5 participates in promoting HSC activation and its expression is significantly down-regulated by VDR activation.

3.4 Promotion of hepatic fibrosis by macrophage exosomal SMAP-5

To verify that SMAP-5 loaded in M2 macrophage exosomes is an essential factor that promotes the activation of HSCs, α-SMA and SMAP-5 were co-stained in liver tissue sections from CCl₄ model mice treated with calcipotriol or GWLP. SMAP-5 was highly expressed through the fibrotic area, confirming that SMAP-5 participated in the progression of hepatic fibrosis in vivo (Fig. 4a). After treatment with calcipotriol, the expression of both α-SMA and SMAP-5 was reduced, while the distribution of α-SMA and SMAP-5 was still obviously co-localized. After treatment with GWLP, the expression of α-SMA was significantly inhibited, but the expression of SMAP-5 was not markedly affected. However, the spread of SMAP-5 was notably blocked, as shown by the lack of co-localization with α-SMA, suggesting the indispensable role of M2 exosomal SMAP-5 in promoting HSC activation. After CCl₄ model mice were treated with calcipotriol and GWLP in combination, despite the significantly repressed α-SMA, both the expression and distribution of SMAP-5 were inhibited, and there was notably less co-localization with α-SMA. To further affirm that the accumulation of SMAP-5 in HSCs was caused by exosomes isolated from M2 macrophages, LX-2 cells were treated with M2 macrophage exosomes and SMAP-5 expression was examined. Results showed that SMAP-5 in LX-2 cells was over-expressed when treated with M2 macrophage exosomes, while the exosomes derived from calcipotriol- or GW4869-treated M2 macrophage had lost this function (Fig. S6a). These results proved that M2 macrophage-derived exosomes enrich the accumulation of SMAP-5 in HSCs.

Then, we explored whether SMAP-5 was the essential effective protein in M2 macrophage exosomes that promoted HSC activation. SMAP-5 was up-regulated using over-expression plasmids in M0 macrophages. The exosomes derived from SMAP-5-over-expressed M0 macrophages were then isolated

(Fig. S6b). When co-cultured with these exosomes, SMAP-5 in LX-2 cells was significantly increased, resulting in higher expression of collagen I and α-SMA (Fig. 4b). To further confirm this result, SMAP-5 was
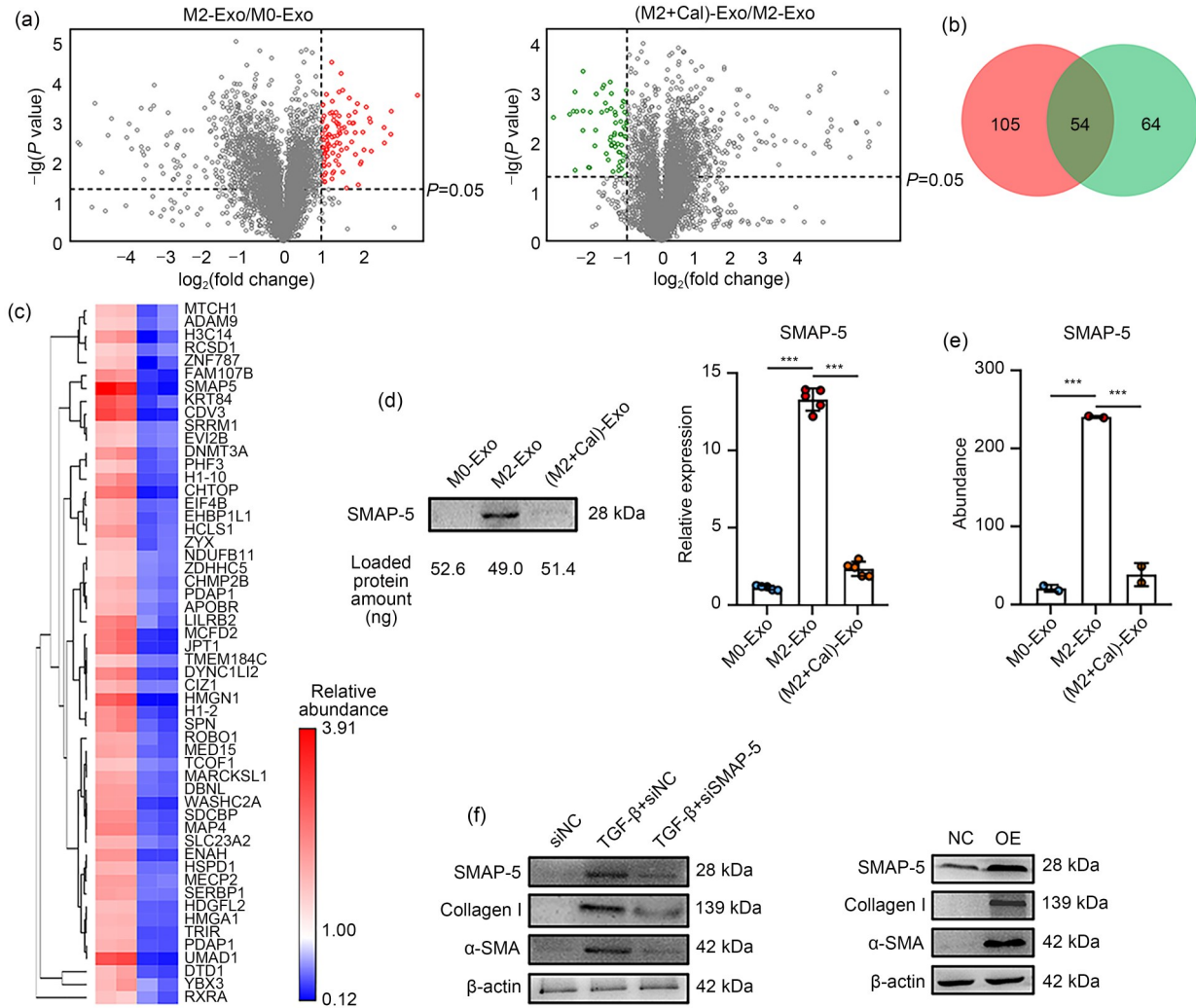

Fig. 3 Proteomic analysis of SMAP-5 as an HSC-activating factor. (a) Volcano diagram of proteins comparing exosomes isolated from THP-1-derived M2 macrophages and M0 macrophages (left). Red dots denote the significant differentially expressed up-regulated proteins. Volcano diagram of proteins comparing exosomes isolated from THP-1-derived calcipotriol-treated M2 macrophages and control M2 macrophages (right). Green dots denote the significant differentially expressed down-regulated proteins. _n_=2. (b) Venn diagram of proteins among significant differentially expressed up-regulated proteins (red) and down-regulated proteins (green) in volcano diagrams. (c) Hierarchical clustering and heatmap analysis of proteins in the intersection of the Venn diagram. _t_ statistics of log$_2$(fold change+1) values of proteins were clustered hierarchically and visualized by heatmap analysis. The red color indicates that the expression of the protein increased in M2-derived exosomes compared to that of M0-derived exosomes, whereas blue indicates that the expression of the protein decreased in calcipotriol-treated M2-derived exosomes compared that of control M2-derived exosomes. (d) Expression of SMAP-5 in exosomes was examined by western blot. Representative gel electrophoresis bands are shown. Protein expression levels were quantified. Numbers under protein bands are estimated protein mass (ng) based on protein standards by BCA assay. Data are expressed as mean±SEM (_n_=5). (e) Quantification of SMAP-5 abundance in exosomes isolated from THP-1-derived M0, M2, and M2+Cal, according to LC-MS/MS results. Data are expressed as mean±SEM (_n_=2). (f) Expression of SMAP-5, collagen I, and α-SMA in LX-2 transfected with siRNA (left) or plasmid (right) was examined by western blot. Representative gel electrophoresis bands are shown. * _P_<0.001. SMAP-5: smooth muscle cell-associated protein 5; HSC: hepatic stellate cell; Exo: exosome; Cal: calcipotriol; BCA: bicinchoninic acid; SEM: standard error of mean; LC-MS/MS: liquid chromatography-tandem mass spectrometry; α-SMA: α-smooth muscle actin; TGF-β: transforming growth factor-β; si: small interfering; NC: negative control; OE: over-expression (Note: for interpretation of the references to color in this figure legend, the reader is referred to the web version of this article).**
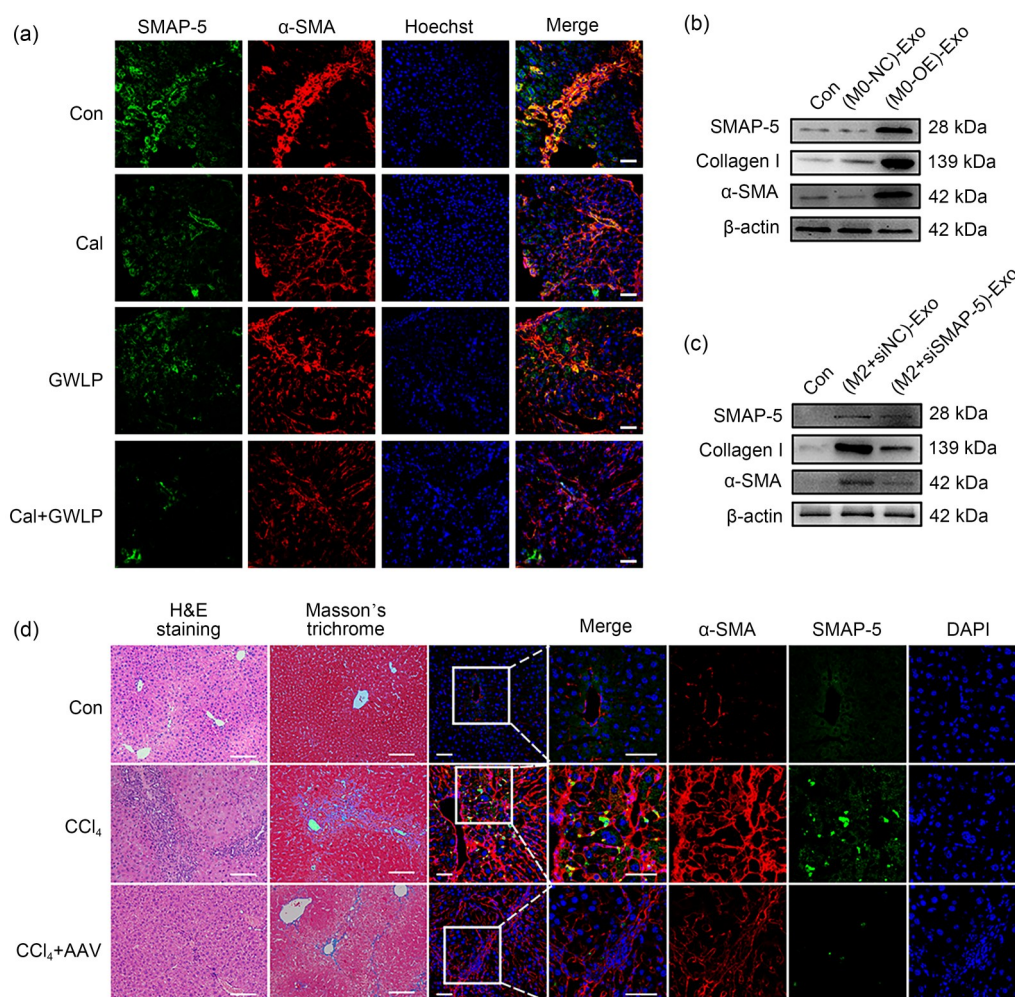
Fig. 4 Promotion of hepatic fibrosis by macrophage exosomal SMAP-5. (a) CLSM images of liver tissue sections from hepatic fibrosis model mice, co-stained for SMAP-5 (green), α-SMA (red), and Hoechst (blue), showed fibrotic area and distribution of SMAP-5. Scale bar=50 μm. (b, c) Expression of SMAP-5, collagen I, and α-SMA in LX-2 treated with different exosomes was examined by western blot. Representative gel electrophoresis bands are shown. (d) Representative images of H&E staining (first column), Masson's trichrome stain (second column), and immunofluorescence (subsequent columns) staining for α-SMA (red), SMAP-5 (green), and DAPI (blue). H&E and Masson's trichrome stain: scale bar= 200 μm; CLSM images: scale bar=50 μm. SMAP-5: smooth muscle cell-associated protein 5; CLSM: confocal laser scanning microscope; α-SMA: α-smooth muscle actin; Cal: calcipotriol; GWLP: GW4869 encapsulated in liposome; Con: control; Exo: exosome; H&E: hematoxylin and eosin; si: small interfering; NC: negative control; OE: over-expression; CCl$_4$: carbon tetrachloride; AAV: adeno-associated virus; DAPI: 4',6-diamidino-2-phenylindole (Note: for interpretation of the references to color in this figure legend, the reader is referred to the web version of this article).

knocked down in M2 macrophages and the SMAP-5-deficient M2 exosomes were isolated (Fig. S6b). After treatment with SMAP-5-deficient M2 exosomes, the expression levels of collagen I and α-SMA in co-cultured LX-2 cells were significantly reduced (Fig. 4c), suggesting that SMAP-5 derived from M2 macrophage exosomes promotes HSC activation.

To demonstrate the essential role of SMAP-5 in hepatic fibrosis in vivo, the AAV-mediated expression of SMAP-5-shRNA (AAV-shSMAP-5) was applied to

hepatic fibrosis model mice at 9.33×10^{12} v. g/kg body weight by vein injection. AAV-shSMAP-5 treatment revealed a significant decrease of F4/80$^+$ SMAP-5$^+$ macrophages, suggesting that the SMAP-5-expressed F4/80$^+$ macrophages were inhibited, and inhibition of hepatic fibrosis in the CCl$_4$-induced mice model. The mice had a well-restored liver tissue structure as shown by H&E staining, much reduced collagen accumulation as shown by Masson's trichrome staining, and much reduced α-SMA protein expression as

shown by immunofluorescence analysis (Figs. 4d and S7a). Also, treatment with AAV-shSMAP-5 caused a significant inhibition of serum ALT, AST, and TBA (Fig. S7b). These results indicated that inhibiting the expression of SMAP-5 can effectively control the process of hepatic fibrosis.

Based on the series experiments performed, we confirmed that SMAP-5 over-expressed in M2 macrophage exosomes is the key protein functioning in HSC activation.

3.5 Down-regulation of macrophage exosomal SMAP-5 by VDR, leading to autophagy flux suppression

To clarify the relationship between SMAP-5 and VDR, CD206 and mothers against decapentaplegic homolog 4 (Smad4) were co-stained in liver tissue sections from CCl₄ model mice, and the distribution of Smad4 in M2 macrophages was tested to affirm the effect of the VDR/SMAP-5 axis. As shown in Fig. 5a, Smad4 was located mainly in the nucleus of macrophages, but mainly in the cytoplasm after treatment with calcipotriol. Then CD206 and SMAP-5 were co-stained to explore the distribution of SMAP-5 in M2 macrophages (Fig. 5b). A series of images showed that, in hepatic fibrosis mice, SMAP-5 was over-expressed in M2 macrophages and significantly inhibited after treatment with calcipotriol, but still spread out in the microenvironment. In contrast, after GWLP treatment, although SMAP-5 expression was not markedly repressed, it was confined to the M2 macrophages. Moreover, combined treatment with calcipotriol and GWLP not only significantly reduced the expression, but also inhibited the spread of SMAP-5, leading to a better anti-fibrosis effect.

SMAP-5 functions in the activation of inositol-requiring enzyme 1 (IRE1) and unfolded protein response (UPR)-induced autophagy (Taguchi et al., 2017). Activation of these signaling pathways up-regulates the expression of anti-apoptotic and autophagy-related proteins, which are increased during HSC activation (Tsuchida and Friedman, 2017). Therefore, we examined the autophagy flux in HSCs after exosome treatment. Treatment with M2 macrophage exosomes or the SMAP-5-over-expressed M0 exosomes resulted in increased messenger RNA (mRNA) expression of autophagy-related 5 (*ATG5*), *ATG7*, and *ATG12* in LX-2 cells (Fig. 5c). In addition, the expression of these genes in LX-2 cells was inhibited by reducing

the expression of SMAP-5 in M2 exosomes. LX-2 cells treated with exosomes derived from M2 macrophages showed increased LC3A/B-II conjugation and decreased p62 expression, and these effects were reversed after calcipotriol treatment (Fig. 5d). Moreover, CLSM images showed that p62 was deficient in LX-2 cells after treatment with conditioned medium of M2 macrophages, but accumulated significantly after treatment with M2 macrophages treated with calcipotriol and GW4869 (Fig. 5e).

These results suggested that exosomal SMAP-5 from M2 macrophages induces autophagy in HSCs, which can be inhibited by a VDR agonist and exosome secretion inhibitor.

4 Discussion

In this study, we showed that VDR activation inhibited the polarization of M2 macrophages, which plays a pivotal role in activating HSCs and promoting hepatic fibrosis. Specifically, we proved that VDR expression was down-regulated when macrophages were polarizing toward the M2 phenotype, and that after activating VDR by calcipotriol, the M2 biomarkers were significantly reduced. Next, to explore the regulation effect of macrophages on HSC activation, LX-2 cells were treated with conditioned medium from different macrophage phenotypes. We found that LX-2 cells were activated when co-cultured with M2 macrophages and the activation of VDR could block this process, revealing that M2 macrophages promoted the activation of HSCs and this regulation was adjusted by VDR activation.

Since it has been proved that macrophages can secrete exosomes to affect the physiological activity of surrounding cells (Chen et al., 2020; Lu et al., 2021), we surmised that the regulation effect of M2 macrophages on HSC activation might be mediated by exosomes. Exosomes are small extracellular vesicles released by various types of cells, which can carry multiple cargos, including proteins, DNA, mRNA, microRNA (miRNA), long non-coding RNA (lncRNA), and lipids (Thery et al., 2018; Kalluri and LeBleu, 2020). Recently, exosomes have drawn significant attention as an essential mediator of intercellular communication in both physiological and pathological conditions (Wang et al., 2023). To demonstrate that
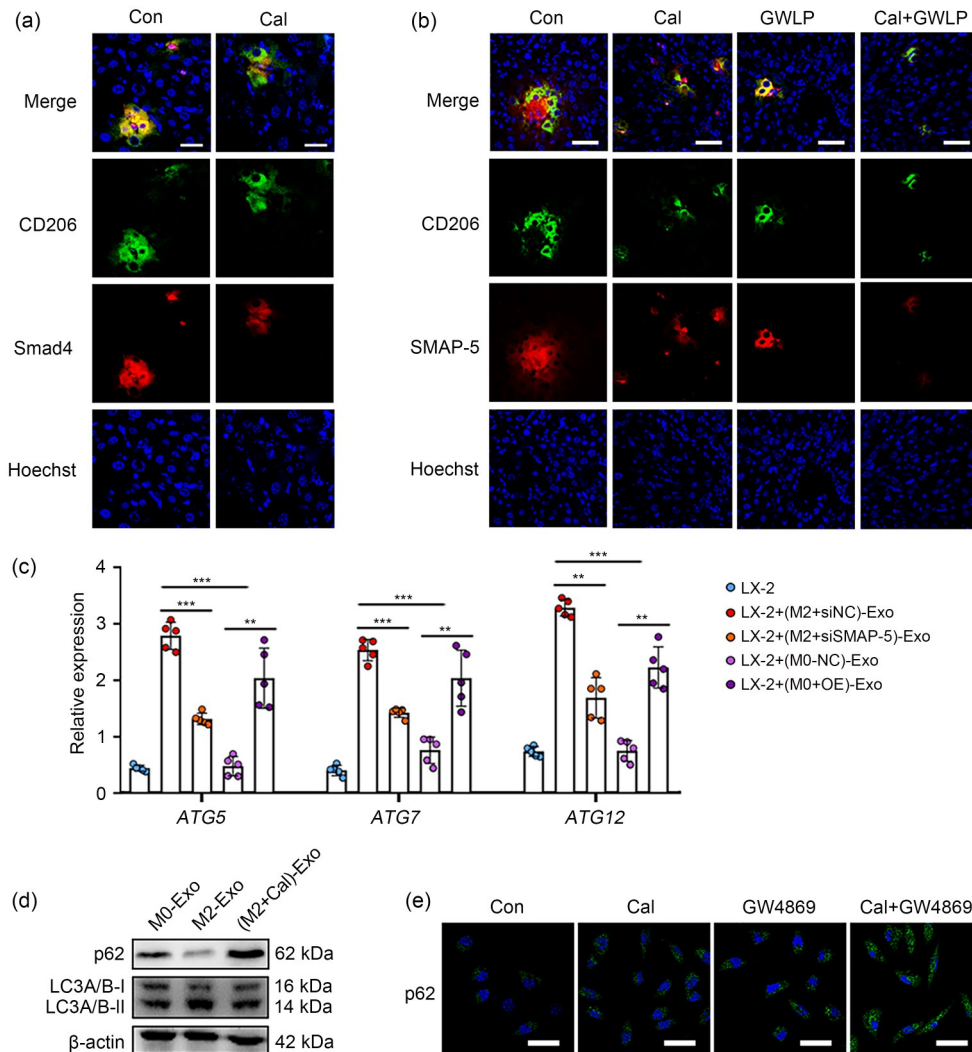
Fig. 5 Down-regulation of macrophage exosomal SMAP-5 by VDR, leading to autophagy flux suppression. (a) CLSM images of liver tissue sections from CCl_4 model mice and calcipotriol-treated CCl_4 mice, co-stained for CD206 (green), Smad4 (red), and Hoechst (blue), showed distribution of Smad4. Scale bar=10 μm. **(b)** CLSM images of liver tissue sections from hepatic fibrosis model mice, treated with Cal, GWLP, or Cal and GWLP combined treatment, co-stained for CD206 (green), SMAP-5 (red), and Hoechst (blue), showed expression and distribution of SMAP-5. Scale bar=10 μm. **(c)** RT-PCR quantification of *ATG5*, *ATG7*, and *ATG12* in LX-2 treated with different exosomes. *U36B4* was used as the control. Data are expressed as mean±SEM (*n*=5). **(d)** Expression of LC3A/B and p62 in LX-2 was examined by western blot. Representative gel electrophoresis bands are shown. **(e)** CLSM images of LX-2 treated with macrophage-conditioned medium, co-stained for p62 (green) and Hoechst (blue). Scale bar=10 μm. ** *P*<0.01, *** *P*<0.001. SMAP-5: smooth muscle cell-associated protein 5; VDR: vitamin D receptor; CLSM: confocal laser scanning microscope; CCl_4: carbon tetrachloride; CD206: cluster of differentiation 206; Smad4: mothers against decapentaplegic homolog 4; GWLP: GW4869 encapsulated in liposome; Cal: calcipotriol; RT-PCR: reverse transcription-polymerase chain reaction; *ATG5*: autophagy-related 5; SEM: standard error of mean; Con: control; Exo: exosome; si: small interfering; NC: negative control; OE: over-expression (Note: for interpretation of the references to color in this figure legend, the reader is referred to the web version of this article).

macrophage-derived exosomes regulate the activation of HSCs, we isolated exosomes from different phenotypes of macrophages and co-cultured them with LX-2 cells. As expected, exosomes derived from M2 macrophages could greatly promote LX-2 cell activation, and this process was inhibited by VDR agonist treatment of M2 macrophages. Moreover, the removal of exosomes in conditioned medium or inhibition of exosome secretion could inhibit the activation of HSCs by M2 macrophages. These data suggest

that, as an essential mediator, exosomes derived from M2 macrophages significantly promote the activation of HSCs.

As widely reported, calcipotriol treatment can significantly inhibit extracellular matrix deposition in liver tissue and decrease AST, ALT, and TBA levels in hepatic fibrosis mice (Ding et al., 2013; Sassi et al., 2018). GWLP treatment alone can also reduce the progress of hepatic fibrosis, while treatment with calcipotriol and GWLP combined can lead to stronger inhibition of fibrosis progression. This in vivo study further confirmed that M2 macrophage-derived exosomes promoted the activation of HSCs. To investigate the key proteins in macrophage exosomes that activate HSCs, 5520 exosomal proteins from M0, M2, and calcipotriol-treated M2 macrophages were identified by LC-MS/MS assay. Statistical analysis showed that particular proteins were notably enriched in M2 macrophage exosomes, and reduced after VDR agonist treatment. Based on a series of experiments, SMAP-5, a protein located in the Golgi complex and which can be transported toward exosomes via the Golgi-to-endosome pathway, was selected (Soonthornsit et al., 2017; Ran et al., 2019).

As SMAP-5 is known to be induced by the TGF-β signal pathway (Stolle et al., 2005), which can be suppressed by VDR activation, the distribution of Smad4 in M2 macrophages was tested to affirm the VDR/SMAP-5 axis. As confirmed, in M2 macrophages infiltrated in an area of hepatic fibrosis, Smad4 translocated into the nucleus and promoted the expression of SMAP-5. Since it has been reported that SMAP-5 can lead to up-regulation of autophagy (Taguchi et al., 2017) and increased autophagy flux can drive HSC activation (Wang, 2015), we surmised that SMAP-5 might promote the activation of HSCs by up-regulation of autophagy. Treatment of HSCs with SMAP-5-enriched M2 exosomes led a much higher autophagy flux and greatly promoted activation. This proved that M2-derived exosomal SMAP-5 is involved in the increased autophagy and activation of HSCs.

As shown in Fig. 6, our study illustrates an essential role of VDR in HSC activation. Mechanistically, M2 macrophages promote HSC activation by secreting SMAP-5-enriched exosomes, a process which is inhibited by activated VDR. Combined treatment with calcipotriol and GWLP achieved an excellent anti-hepatic fibrosis effect that will provide a novel effective strategy for clinical treatment of hepatic fibrosis.

5 Conclusions

This study clarified the effect of M2 macrophages on the activation of HSCs and elucidated the mechanisms of VDR in HSC activation. The results indicated that SMAP-5 is highly expressed in M2 macrophages, and exosomal SMAP-5 can induce HSC activation by increasing autophagy flux. Combined treatment with the VDR agonist calcipotriol and the exosomal secretion inhibitor GW4869 significantly inhibited the hepatic fibrosis. Calcipotriol down-regulates
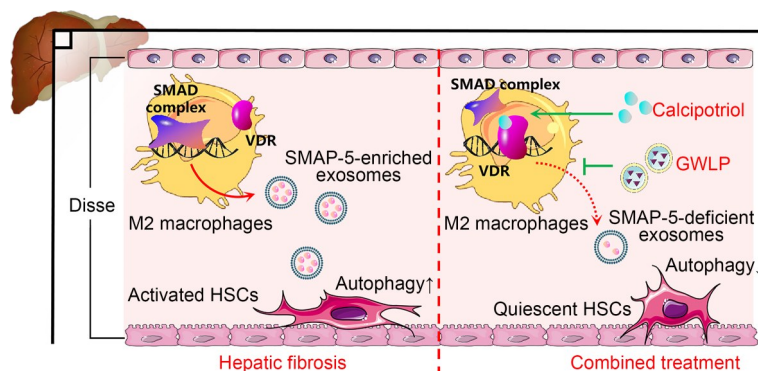

Fig. 6 Schematic illustration of combined treatment of vitamin D receptor (VDR) agonist calcipotriol and macrophage-targeted exosomal secretion inhibitor GW4869 for the treatment of hepatic fibrosis. M2 macrophages secrete smooth muscle cell-associated protein 5 (SMAP-5)-enriched exosomes to promote hepatic stellate cell (HSC) autophagy and activation, which is blocked by activated VDR, providing new targets for intervention in hepatic fibrosis pathogenesis. Combined treatment of calcipotriol and liposome-encapsulated GW4869 (GWLP) shows better curative results, providing a new strategy for clinical treatment of hepatic fibrosis. SMAD: mothers against decapentaplegic.

the expression of exosomal SMAP-5, and GW4869 blocks the transport of SMAP-5 to HSCs via exosomes. Thus, this approach may provide a more effective means for clinical treatment of hepatic fibrosis.

Materials and methods

The detailed methods are provided in the electronic supplementary materials of this paper.

Author contributions

Xuwentai LIU (Conceptualization: equal; Data curation: lead; Formal analysis: equal; Investigation: lead; Methodology: equal; Validation: lead; Visualization: lead; Writing–original draft: lead; Writing–review & editing: equal); Yue WU (Validation: supporting); Yanyi LI (Writing–review & editing: supporting); Kaiming LI (Writing–review & editing: supporting); Siyuan HOU (Conceptualization: supporting; Funding acquisition: supporting; Project administration: supporting; Resources: supporting); Ming DING (Resources: supporting; Visualization: supporting); Jingmin TAN (Methodology: supporting; Visualization: supporting); Zijing ZHU (Methodology: supporting); Yingqi TANG (Methodology: supporting); Yuming LIU (Methodology: supporting); Qianhui SUN (Investigation: supporting); Cong WANG (Conceptualization: lead; Data curation: equal; Formal analysis: lead; Funding acquisition: equal; Methodology: lead; Project administration: lead; Resources: equal; Supervision: lead; Writing–review & editing: lead); Can ZHANG (Funding acquisition: lead; Project administration: equal; Resources: lead; Supervision: equal).

Compliance with ethics guidelines

Xuwentai LIU, Yue WU, Yanyi LI, Kaiming LI, Siyuan HOU, Ming DING, Jingmin TAN, Zijing ZHU, Yingqi TANG, Yuming LIU, Qianhui SUN, Cong WANG, and Can ZHANG declare that they have no conflict of interest.

Informed consent was obtained from all the human blood donors before the experiments were carried out. All experiments were performed in compliance with the Guide for Use of Human Blood and approved by the Ethics Committee of China Pharmaceutical University. All animal experiments were approved by the Animal Experimentation Ethics Committee of China Pharmaceutical University (Approval No. 2021-10-011).

References

Bernsmeier C, van der Merwe S, Périanin A, 2020. Innate immune cells in cirrhosis. *J Hepatol*, 73(1):186-201.
https://doi.org/10.1016/j.jhep.2020.03.027

Cai XP, Cai HQ, Wang J, et al., 2022. Molecular pathogenesis of acetaminophen-induced liver injury and its treatment options. *J Zhejiang Univ-Sci B (Biomed & Biotechnol)*, 23(4):265-285.
https://doi.org/10.1631/jzus.B2100977

Chen LS, Yao XW, Yao HB, et al., 2020. Exosomal miR-103-3p from LPS-activated THP-1 macrophage contributes to the activation of hepatic stellate cells. *FASEB J*, 34(4):5178-5192.
https://doi.org/10.1096/fj.201902307RRR

Ding N, Yu RT, Subramaniam N, et al., 2013. A vitamin D receptor/SMAD genomic circuit gates hepatic fibrotic response. *Cell*, 153(3):601-613.
https://doi.org/10.1016/j.cell.2013.03.028

Dong BN, Zhou Y, Wang W, et al., 2020. Vitamin D receptor activation in liver macrophages ameliorates hepatic inflammation, steatosis, and insulin resistance in mice. *Hepatology*, 71(5):1559-1574.
https://doi.org/10.1002/hep.30937

Duran A, Hernandez ED, Reina-Campos M, et al., 2016. P62/SQSTM1 by binding to vitamin D receptor inhibits hepatic stellate cell activity, fibrosis, and liver cancer. *Cancer Cell*, 30(4):595-609.
https://doi.org/10.1016/j.ccell.2016.09.004

Hu MY, Wang Y, Liu ZS, et al., 2021. Hepatic macrophages act as a central hub for relaxin-mediated alleviation of liver fibrosis. *Nat Nanotechnol*, 16(4):466-477.
https://doi.org/10.1038/s41565-020-00836-6

Kalluri R, LeBleu VS, 2020. The biology, function, and biomedical applications of exosomes. *Science*, 367(6478):eaau6977.
http://doi.org/10.1126/science.aau6977

Kisseleva T, Brenner D, 2021. Molecular and cellular mechanisms of liver fibrosis and its regression. *Nat Rev Gastroenterol Hepatol*, 18(3):151-166.
https://doi.org/10.1038/s41575-020-00372-7

Konstantakis C, Tselekouni P, Kalafateli M, et al., 2016. Vitamin D deficiency in patients with liver cirrhosis. *Ann Gastroenterol*, 29(3):297-306.
https://doi.org/10.20524/aog.2016.0037

Li PF, Ma C, Li J, et al., 2022. Proteomic characterization of four subtypes of M2 macrophages derived from human THP-1 cells. *J Zhejiang Univ-Sci B (Biomed & Biotechnol)*, 23(5):407-422.
https://doi.org/10.1631/jzus.B2100930

Liu PT, Stenger S, Li HY, et al., 2006. Toll-like receptor triggering of a vitamin D-mediated human antimicrobial response. *Science*, 311(5768):1770-1773. https://doi.org/10.1126/science.1123933

Lu ZN, Niu WX, Zhang N, et al., 2021. Pantoprazole ameliorates liver fibrosis and suppresses hepatic stellate cell activation in bile duct ligation rats by promoting YAP degradation. *Acta Pharmacol Sin*, 42(11):1808-1820. https://doi.org/10.1038/s41401-021-00754-w

Mokdad AA, Lopez AD, Shahraz S, et al., 2014. Liver cirrhosis mortality in 187 countries between 1980 and 2010: a systematic analysis. *BMC Med*, 12:145. https://doi.org/10.1186/s12916-014-0145-y

Pellicoro A, Ramachandran P, Iredale JP, et al., 2014. Liver fibrosis and repair: immune regulation of wound healing in a solid organ. *Nat Rev Immunol*, 14(3):181-194. https://doi.org/10.1038/nri3623

Qu C, Zheng DD, Li S, et al., 2018. Tyrosine kinase SYK is a potential therapeutic target for liver fibrosis. *Hepatology*, 68(3):1125-1139. https://doi.org/10.1002/hep.29881

Ran Y, Xiong MG, Xu ZS, et al., 2019. YIPF5 is essential for innate immunity to DNA virus and facilitates COPII-dependent STING trafficking. *J Immunol*, 203(6):1560-1570. https://doi.org/10.4049/jimmunol.1900387

Sassi F, Tamone C, D'Amelio P, 2018. Vitamin D: nutrient, hormone, and immunomodulator. *Nutrients*, 10(11):1656. https://doi.org/10.3390/nu10111656

Seki E, Schwabe RF, 2015. Hepatic inflammation and fibrosis: functional links and key pathways. *Hepatology*, 61(3):1066-1079. https://doi.org/10.1002/hep.27332

Shen DF, Cheng H, Cai BZ, et al., 2022. *N*-n-Butyl haloperidol iodide ameliorates liver fibrosis and hepatic stellate cell activation in mice. *Acta Pharmacol Sin*, 43(1):133-145. https://doi.org/10.1038/s41401-021-00630-7

Shen ZR, Shao JJ, Sun JQ, et al., 2022. Exosomes released by melanocytes modulate fibroblasts to promote keloid formation: a pilot study. *J Zhejiang Univ-Sci B (Biomed & Biotechnol)*, 23(8):699-704. https://doi.org/10.1631/jzus.B2200036

Sica A, Invernizzi P, Mantovani A, 2014. Macrophage plasticity and polarization in liver homeostasis and pathology. *Hepatology*, 59(5):2034-2042. https://doi.org/10.1002/hep.26754

Soonthornsit J, Sakai N, Sasaki Y, et al., 2017. YIPF1, YIPF2, and YIPF6 are *medial-/trans*-Golgi and *trans*-Golgi network-localized Yip domain family proteins, which play a role in the Golgi reassembly and glycan synthesis. *Exp*

Cell Res, 353(2):100-108. https://doi.org/10.1016/j.yexcr.2017.03.011

Stolle K, Schnoor M, Fuellen G, et al., 2005. Cloning, cellular localization, genomic organization, and tissue-specific expression of the TGFβ1-inducible *SMAP-5* gene. *Gene*, 351:119-130. https://doi.org/10.1016/j.gene.2005.03.012

Sun YY, Li XF, Meng XM, et al., 2017. Macrophage phenotype in liver injury and repair. *Scand J Immunol*, 85(3):166-174. https://doi.org/10.1111/sji.12468

Taguchi Y, Horiuchi Y, Kano F, et al., 2017. Novel prosurvival function of Yip1A in human cervical cancer cells: constitutive activation of the IRE1 and PERK pathways of the unfolded protein response. *Cell Death Dis*, 8(3):e2718. https://doi.org/10.1038/cddis.2017.147

Thery C, Witwer KW, Aikawa E, et al., 2018. Minimal information for studies of extracellular vesicles 2018 (MISEV2018): a position statement of the International Society for Extracellular Vesicles and update of the MISEV2014 guidelines. *J Extracell Vesicles*, 7(1):1535750. http://doi.org/10.1080/20013078.2018.1535750

Tsuchida T, Friedman SL, 2017. Mechanisms of hepatic stellate cell activation. *Nat Rev Gastroenterol Hepatol*, 14(7):397-411. https://doi.org/10.1038/nrgastro.2017.38

Wang KW, 2015. Autophagy and apoptosis in liver injury. *Cell Cycle*, 14(11):1631-1642. https://doi.org/10.1080/15384101.2015.1038685

Wang XP, Wang GY, Qu JW, et al., 2020. Calcipotriol inhibits NLRP3 signal through YAP1 activation to alleviate cholestatic liver injury and fibrosis. *Front Pharmacol*, 11:200. https://doi.org/10.3389/fphar.2020.00200

Wang ZL, Yang JJ, Sun XH, et al., 2023. Exosome-mediated regulatory mechanisms in skeletal muscle: a narrative review. *J Zhejiang Univ-Sci B (Biomed & Biotechnol)*, 24(1):1-14. https://doi.org/10.1631/jzus.B2200243

Yin CY, Evason KJ, Asahina K, et al., 2013. Hepatic stellate cells in liver development, regeneration, and cancer. *J Clin Invest*, 123(5):1902-1910. https://doi.org/10.1172/JCI66369

Zhou Y, Dong BN, Kim KH, et al., 2020. Vitamin D receptor activation in liver macrophages protects against hepatic endoplasmic reticulum stress in mice. *Hepatology*, 71(4):1453-1466. https://doi.org/10.1002/hep.30887

Supplementary information
Materials and methods; Table S1; Figs. S1–S7